RESEARCH ARTICLE

AMERICAN JOURNAL OF BOTANY

Spatiotemporal features of microsporogenesis in the cycad species *Macrozamia communis*[1]

Xiaodong Yan[2], Mei Bai[2], Xiping Ning[2], Haibo Ouyang[3], Shouzhou Zhang[4], Ming Yang[5,7], and Hong Wu[2,6,7]

PREMISE OF THE STUDY: Spatiotemporal features of microsporogenesis may provide important clues about the evolution of microsporogenesis in seed plants. One cellular feature that attracts special attention is advance cell wall ingrowths (ACWIs) at future cytokinetic sites in microsporocytes since they have been found only in species of an ancient lineage of angiosperms, *Magnolia*, and in much less detail, of an ancient lineage of gymnosperms, cycads. Further investigation into microsporogenesis in a cycad species may yield knowledge critical to understanding the establishment of ACWIs as an important feature for comparative studies of microsporogenesis in seed plants.

METHODS: Bright-field and epifluorescence microscopy, confocal laser scanning microscopy, and transmission electron microscopy were used to investigate the microsporogenic process in *Macrozamia communis*, a species in the Zamiaceae family of cycads.

KEY RESULTS: In prophase-II microsporocytes in *M. communis*, ACWIs form as a callose ring between the newly formed nuclei and are not accompanied by cytokinetic apparatuses such as mini-phragmoplasts, wide tubules, or wide tubular networks. Shortly after the second nuclear division, new ACWIs, albeit thinner than the previous ACWIs, form between the newly formed nuclei. Subsequent cell plate formation in the planes of the ACWIs typically results in tetragonal tetrads.

CONCLUSIONS: Cytokinesis at the cell periphery is initiated earlier than cell plate formation in the cell interior in microsporogenesis in *M. communis*. The cellular features uncovered in *M. communis* may serve as useful reference features for comparative studies of microsporogenesis in plants.

KEY WORDS callose; cycads; cytokinesis; evolution; *Macrozamia communis*; *Magnolia*; microsporogenesis; seed plants; Zamiaceae

Cytokinesis is a spatially and temporally regulated process through which the cellular components of a mother cell are partitioned into daughter cells, resulting in an increase in cell number (Balasubramanian et al., 2004). In animal and fungal cells, cytokinesis is accomplished through the action of an actomyosin-based contractile ring that cleaves the cytoplasm (Glotzer, 1997; Field et al., 1999). Cytokinesis in plant cells, on the other hand, takes place without such a contractile ring; it is accomplished by a common mechanism of fusion of phragmoplast-delivered vesicles at the division plane even though the details in the steps leading to the completion of cytokinesis may vary in different cell types (Gunning, 1982; Jürgens, 2005).

It is generally accepted that there are three types of cytokinesis in microsporogenesis in seed plants, which may have an implication on the evolution of microsporogenesis in seed plants (Nadot et al., 2008). The first type is simultaneous cytokinesis that is defined by one cytokinetic event after the second nuclear division. The second type is successive cytokinesis that is characterized by two cytokinetic events with one following each of the two nuclear divisions. The third type is intermediate cytokinesis, during which advance cell wall ingrowths (ACWIs) form at a future cytokinetic site after the first nuclear division, but further cytoplasm partitioning by the cell plates only occurs after the second nuclear division. In all angiosperms investigated, simultaneous cytokinesis is the predominant type in microsporogenesis, while successive cytokinesis mostly occurs in monocot species (Furness et al., 2002; Nadot et al., 2008; Brown and Lemmon, 2013). Intermediate cytokinesis, on the other hand, has been described in detail only in *Magnolia* (Farr, 1918;

[1] Manuscript received 19 March 2015; revision accepted 10 June 2015.

[2] State Key Laboratory for Conservation and Utilization of Subtropical Agro-bioresources, Guangzhou 510642, China;

[3] Fujian Institute of Subtropical Botany, Xiamen 361006, China;

[4] Shenzhen Fairylake Botanical Garden, Shenzhen 518004, China;

[5] Department of Botany, Oklahoma State University, 301 Physical Sciences, Stillwater, Oklahoma 74078 USA; and

[6] Guangdong Key Laboratory for Innovative Development and Utilization of Forest Plant Germplasm, Guangzhou 510642, China

[7] Authors for correspondence (e-mails: ming.yang@okstate.edu, wh@scau.edu.cn)

doi:10.3732/ajb.1500112

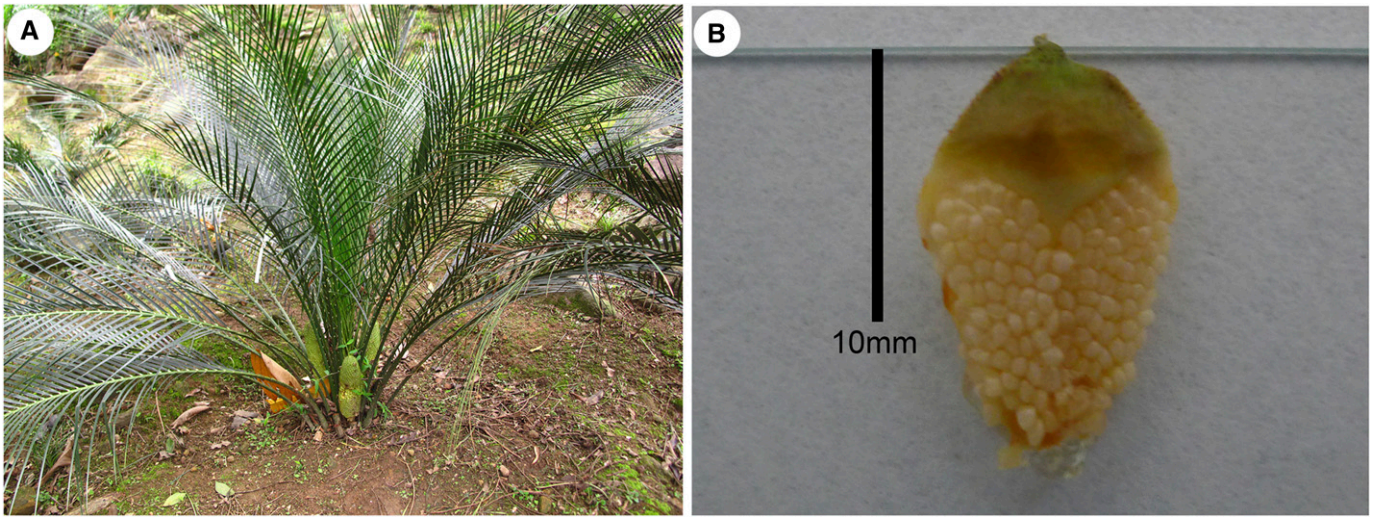

FIGURE 1 Plant and microsporophyll of *Macrozamia communis*. (A) Plant with male cones. (B) Microsporophyll with microsporangia on its abaxial side. For convenience of photographing, the thorn at the tip of microsporophyll was cut off.

Sampson, 1969a, b; Brown and Lemmon, 1992; Nadot et al., 2008). For a comparison, either simultaneous or successive cytokinesis was reported for microsporogenesis in gymnosperm species other than cycads (Maheshwari, 1935; Moitra and Bhatnagar, 1982; Anderson and Owens, 2000; Lü et al., 2003; Zhang et al., 2008; Lu et al., 2011). Currently, only limited information is available on the process of microsporogenesis in several cycads, but the cytokinetic process seems to be similar to the intermediate type (Singh, 1978; Audran, 1981; Zhang et al., 2012).

Simultaneous cytokinesis has been proposed to be an ancestral feature of microsporogenesis in angiosperms and perhaps in all seed plants on the basis of a phylogenetic analysis using cytokinesis type, mode of intersporal wall formation, and tetrad form (Nadot et al., 2008). However, whether the ACWIs in intermediate cytokinesis are an ancestral feature of microsporogenesis of seed plants remains an open question. This question deserves attention since the plant groups known for this feature, *Magnolia* and cycads, are generally recognized as ancient lineages of seed plants (Bowe et al., 2000; Chaw et al., 2000; Sauquet et al., 2003; Brenner et al., 2003), and some seed plant outgroups such as bryophytes (Brown and Lemmon, 2013) and *Dryopteris borreri* (a fern species) (Sheffield et al., 1983) also have ACWIs in sporogenesis. ACWIs in bryophytes typically result in quadrilobed sporocytes before the first nuclear division, and callose is preferentially deposited at the furrows between the adjacent lobes that seem to be specified by the cytoskeleton (Mineyuki, 1999; Pickett-Heaps et al., 1999; Brown and Lemmon, 2001, 2013). ACWIs, therefore, may be another ancient feature of microsporogenic cytokinesis, in addition to the one-time cell plate formation after the second nuclear division as defined in simultaneous cytokinesis.

Even though AWCIs have been reported in microsporogenesis in some cycads, there are still important unanswered questions about the AWCIs. In particular, precisely when the AWCIs are formed during meiosis, whether phragmoplasts are involved in the formation of the AWCIs, and whether two rounds of AWCIs, respectively, follow the two rounds of nuclear divisions are unknown. Categorization of these details of microsporogenesis in a cycad will provide a better reference point for comparative studies of microsporogenesis in seed plants. Here, we report the spatiotemporal features of microsporogenesis in the cycad species *Macrozamia communis* L.A.S.Johnson (Zamiaceae), which show that each of the two nuclear divisions is followed by a separate round of phragmoplast-independent ACWIs. We also discuss the phenomenon of ACWIs in the context of the evolution of microsporogenesis in seed plants.

MATERIALS AND METHODS

***Plant materials*—**The microsporophylls were from a single 15-yr-old individual of *M. communis* cultivated in the Cycad Conservation Center, Shenzhen Fairylake Botanical Garden (Shenzhen, China). From the middle region of the same male cone, 1–2 microsporophylls were repeatedly collected every 1–2 d from April to May and immediately fixed in 4% v/v glutaraldehyde plus 3% w/v paraformaldehyde in 0.2 mol/L phosphate-buffered solution (PBS) at pH 7.2 for more than 4 h.

***Semithin sections*—**After three washes in PBS, the fixed specimens were postfixed in 2% w/v osmium tetroxide in 0.2 mol/L PBS for 3 h at room temperature, followed by three washes in PBS. The specimens were then dehydrated in a graded ethanol series and infiltrated with Epon 812 (SPI Supplies Division of Structure Probe, West Chester, Pennsylvania, USA). Polymerization proceeded for 24 h at 40°C, followed by 24 h at 60°C. Semithin sections (1–2 μm thick) were cut using either a Reichert-Jung or a Leica RM 2155 microtome. Sections were stained with either 0.05% w/v toluidine blue O (TBO), periodic acid–Schiff's reagent and 0.25% haematoxylin, or 1 μg/mL 4′,6-diamidino-2-phenylindole (DAPI) and 0.005% aniline blue (Zhang et al., 2012). Sections were examined and photographed using a Leica DMLB light microscope for both bright-field microscopy and epifluorescence microscopy with the UV channel.

***Ultrathin sections*—**On the basis of the results from the semithin sections, 70–90-nm thick sections were also cut with a diamond knife (Ultra 45, Diatome Ltd., Biel, Switzerland) using a Leica EM

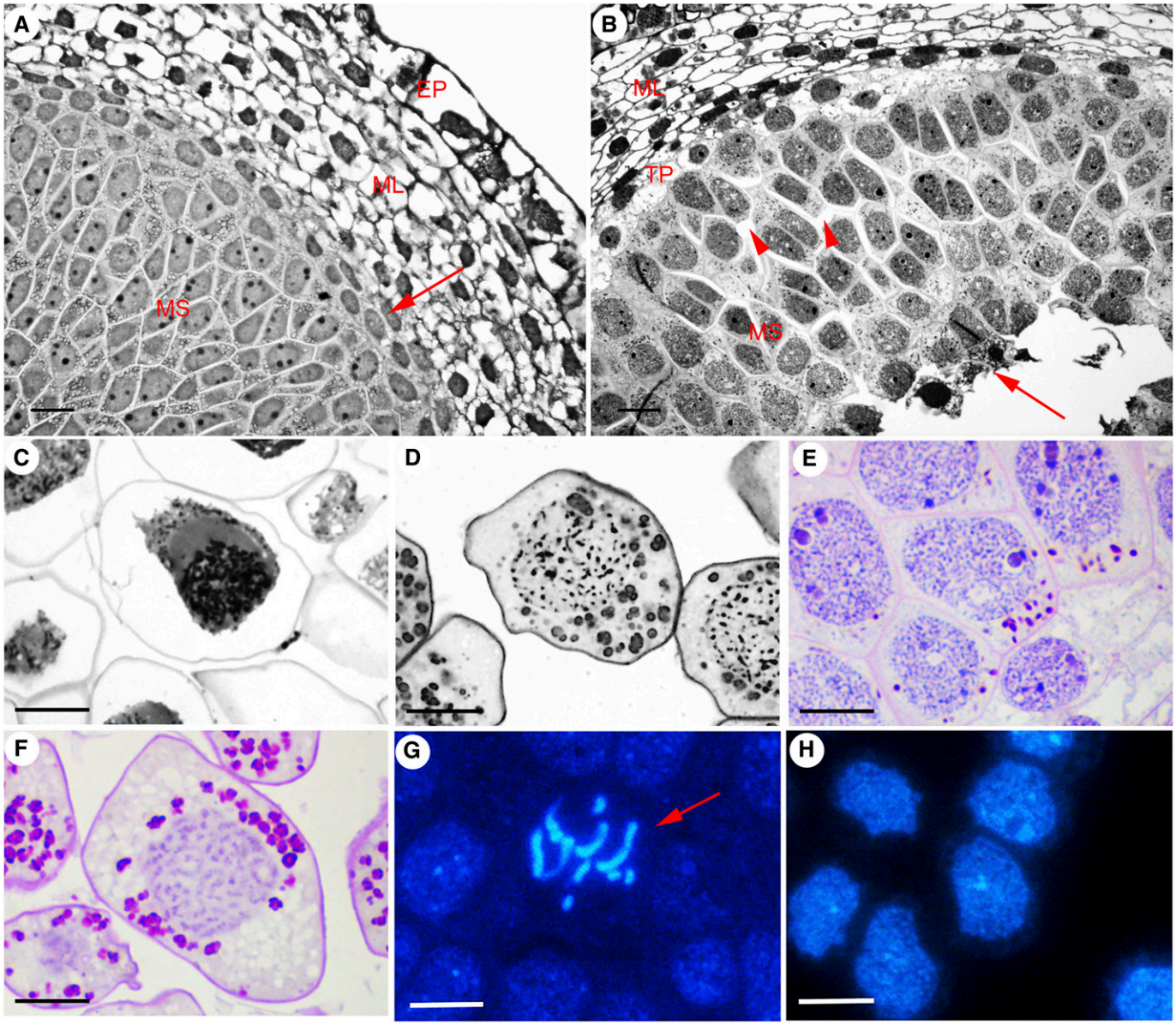

FIGURE 2 Microsporangia and microsporocytes before and during prophase I. (A–D) Semithin sections that were stained with toluidine blue O. (A) Developing microsporangium before prophase I when chromatin in nuclei in the microsporocytes was not condensed. Arrow indicates the tapetum. (B) Wall of microsporangium at meiosis I. Gaps had formed between microsporocytes (arrowheads), and some interior cells had degenerated (arrow). (C) Separating microsporocytes, likely at early prophase I based on the polarized distribution of the nucleus and the organelles (dark granules) in the cell although no apparent chromatin condensation can be seen. At this stage, the microsporocytes were sensitive to changes in osmotic pressure during sample processing so that plasmolysis occurred. (D) Largely separate microsporocytes at a prophase-I stage later than in (C), with a moderate level of chromatin condensation in the nucleus. (E, F) Semithin sections stained with PAS reagent and haematoxylin. (E) Early prophase-I microsporocytes containing starch grains (red as a result of the PAS reaction) at one pole of the cell and partially condensed chromatin (blue dots and fragments from haematoxylin staining) in the nuclei. (F) Microsporocytes likely at the pachytene stage; starch grains were no longer at one pole of the cell, and evenly thick chromosomes threads had appeared. These prophase-I stages were deciphered largely based on well-documented prophase-I features of *Arabidopsis* male meiosis (Wang and Yang, 2014). (G, H) Fluorescence images of semithin sections. (G) DAPI-stained chromosomes (arrow) at late prophase I. (H) Aniline blue-stained cells showing the lack of callose deposition in the walls of microsporocytes at a stage similar to that in (H). EP: epidermis; ML: middle layer; MS: microsporocyte; TP: tapetum. Scale bars = 10 μm.

UC6 ultramicrotome, and collected on 50-mesh copper grids. After staining with uranyl acetate and lead citrate, the sections were observed and photographed using a transmission electron microscope (Philips FEI-TECNAI 12).

Squash method and confocal laser scanning microscopy (CLSM)— Fixed microsporophylls were squashed on a slide in a staining solution containing 50 μg/mL propidium iodide (PI) and 0.005% aniline blue to release and stain individual microsporocytes or

tetrads. After staining for 3 min, observation and photographing were carried out using a ZEISS 780 confocal laser scanning microscope, with the laser wavelengths of 530 nm and 400 nm for PI and aniline blue, respectively. The images were processed using the software Carl Zeiss Zen 2010.

RESULTS

Male cone development and morphology of microsporocytes before the first nuclear division—Development of male cones of *M. communis* started from late March to early April and reached maturity in mid-May. During development, the male cones with cuneiform-shaped microsporophylls gradually emerged from underground and increased in size (Fig. 1A). A large number of microsporangia developed on the abaxial surface of the microsporophyll in an asynchronous fashion (Fig. 1B). At the earliest stage in our samples, the developing microsporangium consisted of the epidermis, the endothecium just underneath the epidermis, the middle layer with multiple cell layers, the tapetum with 1–2 cell layers, and the microsporocytes (Fig. 2A). The microsporocytes were roughly isodiametric, and had straight walls, dense cytoplasm, and a large nucleus with several nucleoli, which clearly distinguished them from the cells in the microsporangial wall. Such morphological differences were more pronounced at a later developmental stage, when the microsporocytes began to separate from one another and the centrally localized cells underwent degradation (Fig. 2B). The intercellular spaces between microsporocytes increasingly enlarged with further development, and the microsporocytes largely separated from one another before the first nuclear division (Fig. 2C, D). During the separation of microsporocytes, the starch grains in plastids were first seen at one pole of the cell (Fig. 2C, E) and later around the nucleus (Fig. 2D, F). In some of the separated microsporocytes, scattered chromosomes were observed with fluorescence microscopy (Fig. 2G), suggesting that these cells were in late prophase I. Whereas large amounts of callose are present in the walls of prophase-I microsporocytes in angiosperms (Worrall et al., 1992), there was little callose deposition in the walls of these cells at this stage (Fig. 2H).

In the angiosperm species *Arabidopsis thaliana*, the separation process of the microsporocytes largely coincides with the progression of prophase I (Wang and Yang, 2006). To determine whether a similar coincidence also occurs in *M. communis*, we investigated chromatin condensation in nonseparating and separating microsporocytes using transmission electron microscopy. Chromatin appeared to be condensed in both the nonseparating (Fig. 3A) and separating (Fig. 3B) microsporocytes examined, with the separating microsporocytes containing more condensed chromatin than the nonseparating microsporocytes. In both types of cells, the nuclear envelope was intact, indicating that they were in relatively early and late prophase I, respectively. The progression of prophase I in *M. communis*, therefore, also coincides with the separation of microsporocytes.

Initiation of cytokinesis at prophase II—There is no indication of cytokinesis in meiosis I (Figs. 2, 3, 4A–C, 4H, 4I). However, in prophase II, when the organelle band had formed between the two nuclei and the chromosomes were undergoing condensation, callose was almost exclusively deposited at the region of the cell wall that was aligned with the organelle band. A positive PAS reaction

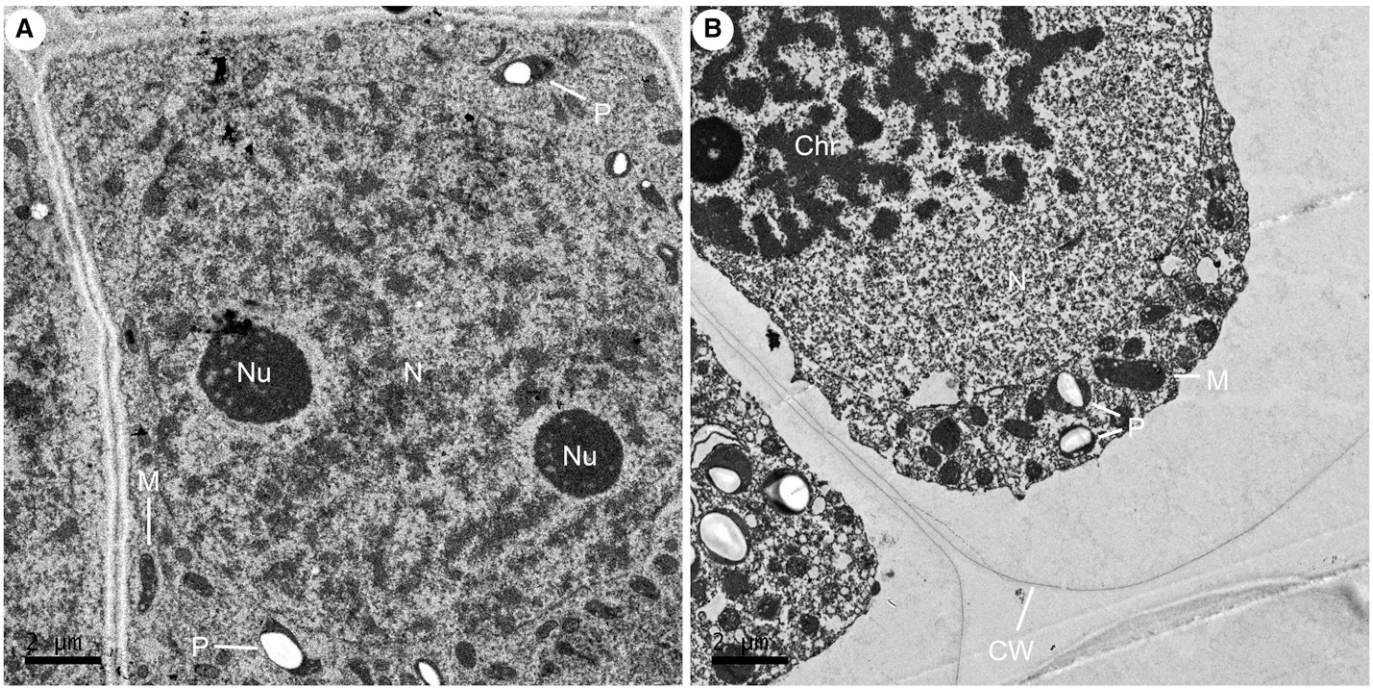

FIGURE 3 Transmission electron micrographs of microsporocytes at prophase I. (A) Microsporocytes at early prophase I with somewhat condensed chromatin and small intercellular spaces. (B) Microsporocytes at a prophase-I stage later than that in (A) with highly condensed chromatin and increasingly large intercellular spaces. Plasmolysis occurred at this stage. Chr: chromosome; CW: cell wall; M: mitochondrion; N: nucleus; Nu: nucleolus; P: plastid.

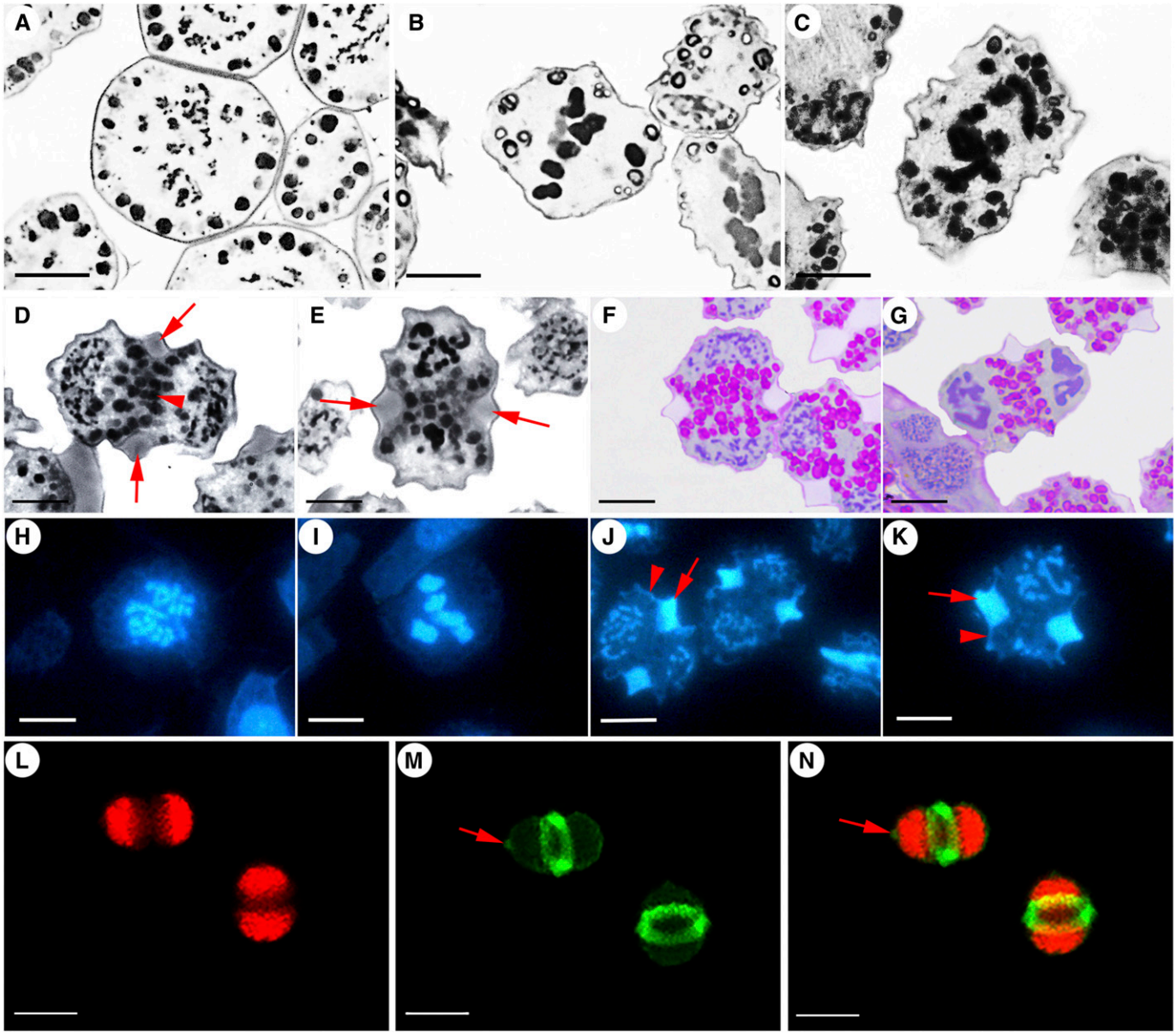

FIGURE 4 Microsporocytes at stages from prophase I to prophase II. (A–E) Semithin sections stained with toluidine blue O. (A) At pachytene or early diplotene, centrally localized nuclei contained condensed chromatin, and the organelles did not have a polarized distribution. (B) Metaphase I; chromosomes aligned at the equatorial plane. (C) At anaphase I, segregated homologous chromosomes had moved toward opposite poles. Cell walls were uniformly thin at this stage. (D) At early prophase II, the organelle band (arrowhead) was at the equatorial plane of the cell, which separated the two nuclei that contained condensed chromatin. Strikingly, two areas of cell wall thickening appeared at the site where the organelle band intercepted the cell periphery (arrows). (E) At late prophase II, condensed chromosomes appeared, and the two thickened wall areas seemed to be more enlarged and to have invaded farther into the cytoplasm than in (D). However, the two thickened wall areas never extended to form a continuous wall, i.e., the microsporocytes did not become dyads at this stage. (F, G) Semithin sections after PAS and haematoxylin staining. Sections in (F) and (G) are at stages comparable to those in (D) and (E), respectively. The organelle band was dominated by starch-containing plastids according to the result of the PAS reaction. (H–K) Semithin sections stained with DAPI and aniline blue. (H) At pachytene or diplotene, thick chromosome threads appeared; the cell wall did not have apparent callose deposition. (I) At metaphase I, homologous chromosomes aligned at the equatorial plane; the cell wall did not have apparent callose deposition. (J, K) Stages similar to those in (D) and (E), respectively. The cell wall thickening areas contained callose (arrows), and callose was also deposited laterally away from the thickened areas to a limited extent (arrowhead). (L–N) Images constructed by stacking the *z*-series of CLSM images, showing a three-dimensional view of callose deposition. (L) Propidium iodide staining, showing the nuclei at prophase II. (M) Aniline blue staining (false-colored to green), showing callose deposition throughout the wall of the same cell in (L). A callose ring had clearly been deposited around the mid-region of the cell relative to the two nuclei at either pole. Additional small wall areas also had localized callose deposition (arrow) at this stage; these areas seemed to foretell the location of the second callose ring that would emerge after the second nuclear division (see Fig. 7). (N) Image of merged (L) and (M). Scale bars: A–K = 10 μm; L–N = 20 μm.

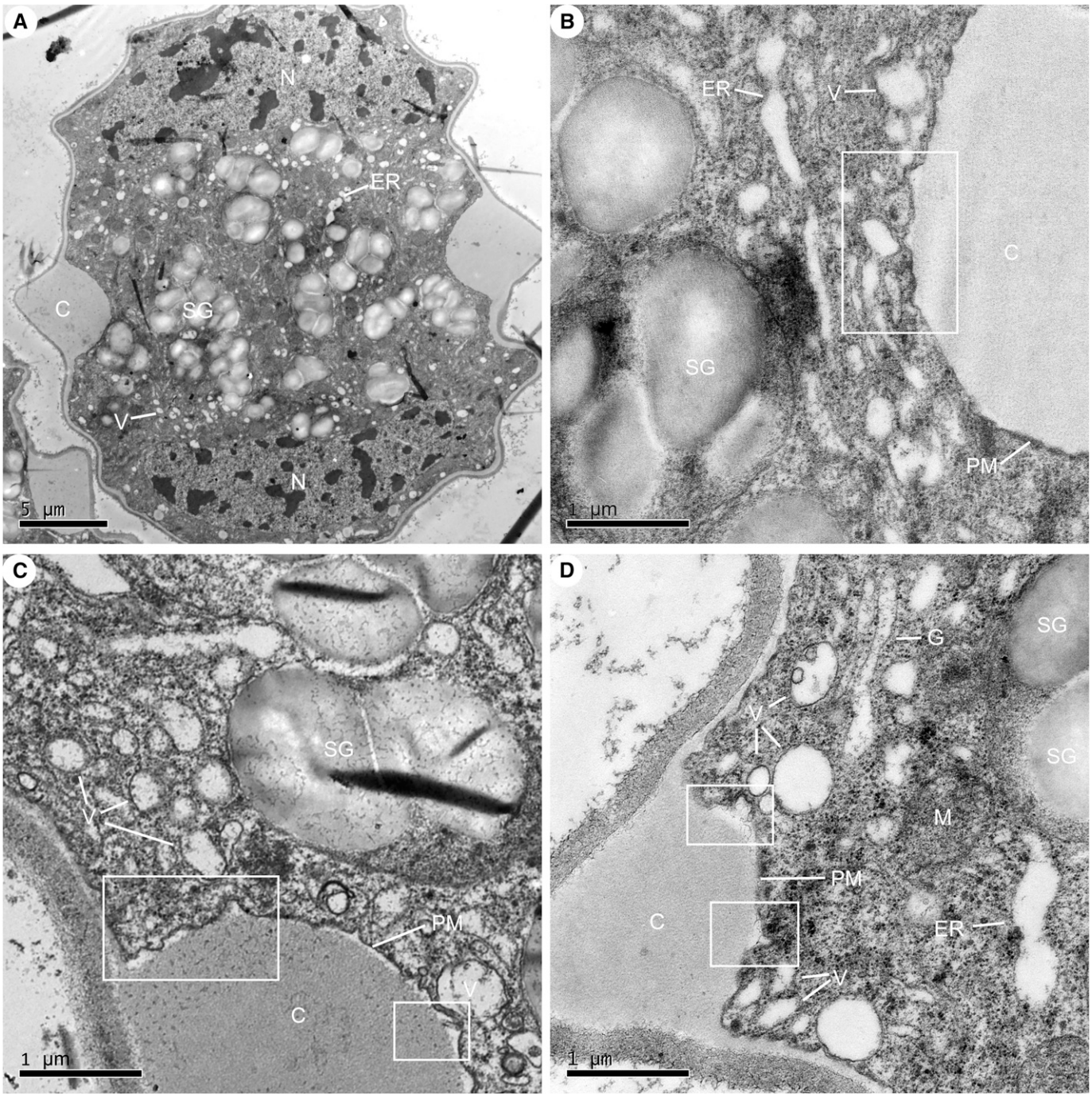

FIGURE 5 (A–D) Electron micrographs of microsporocytes at prophase II. (A) View of callose ring in cross section. (B–D) Inner side of the callose ring had projections into the cytoplasm that was rich in vesicles, ER and Golgi bodies. The projections from the callose ring are more electron-translucent than the rest of the callose ring, and their electron density is similar to that of the vesicles nearby (rectangles). C: callose ring; ER: endoplasmic reticulum; G: Golgi body; M, mitochondrion; N: nucleus; PM: plasma membrane; SG: starch grain; V: vesicle.

indicated that the organelle band consisted primarily of starch-containing plastids (Fig. 4F, G). The callose deposition had somewhat pointed ends toward both the outside and inside of the cell, creating an appearance of a cytoplasmic furrow, but callose deposition never progressed to form a continuous wall that would have partitioned the cytoplasm into two cells at this stage. Rather, the consistent presence of such callose deposition on all cells observed at this stage suggests that the callose forms a ring structure. To demonstrate the existence of such a callose ring, we used CLSM to create three-dimensional views of the callosic structure. Indeed, a thick callose ring was observed in the equatorial plane at prophase II, along with much less callose deposition elsewhere in the cell wall (Fig. 4L–N).

These observations raised the possibility that cytokinesis started and underwent limited progression during prophase II. To further

investigate the cytokinetic process, we examined the morphology of microsporocytes in prophase II using transmission electron microscopy. At its leading edges protruding into the cytoplasm, the callose ring contained small projections that were more electron-translucent than the other region of the callose ring (Fig. 5A–D). There were abundant electron-translucent vesicles near the small projections in the cytoplasm. It is reasonable to assume that fusions of these vesicles with the plasma membrane resulted in the formation of the callose ring (Fig. 5B–D). The callose ring with the small projections resembles the cell wall stub with convoluted sheets at the leading edges of the stub in cytokinesis in *Arabidopsis* microsporogenesis as described by Otegui and Staehelin (2004). However, at this stage in *M. communis*, we did not observe structures similar to those in the cytokinesis in *Arabidopsis* microsporogenesis, i.e., mini-phragmoplasts, wide tubules, and wide tubular networks, which all form within a short time along with the stub in events that quickly lead to the formation of a complete cell plate (Otegui and Staehelin, 2004). Except for a slight increase in the thickness of the callose ring, no other progress in cytokinesis was observed during the subsequent period from metaphase II to early telophase II (Fig. 6). Cytokinesis in microsporogenesis in *M. communis*, therefore, starts around prophase II at the cell periphery but does not initiate the process of cell plate formation in the cell interior up to the stage as late as telophase II.

***Resumption and completion of cytokinesis*—**Observations with CLSM indicated that cytokinesis resumed after telophase II at two division planes that coincided with the previously formed callose ring and a newly formed callose ring, respectively (Fig. 7). Two callose rings without complete new cell walls were observed in some microsporocytes (Figs. 7D–F, 8A), suggesting that the second callose ring also formed before the formation of the corresponding cell wall. The callose wall from the first callose ring was much thicker than that from the second callose ring (Figs. 7A–C, 7G–I, 9A–F). Tetragonal tetrads were typically produced as a result of the cytokinesis (Figs. 7A–C, 7G–I, 9A–F).

As seen with TEM, when both callose rings were present but mature cell walls were absent in a microsporocyte, cellular structures

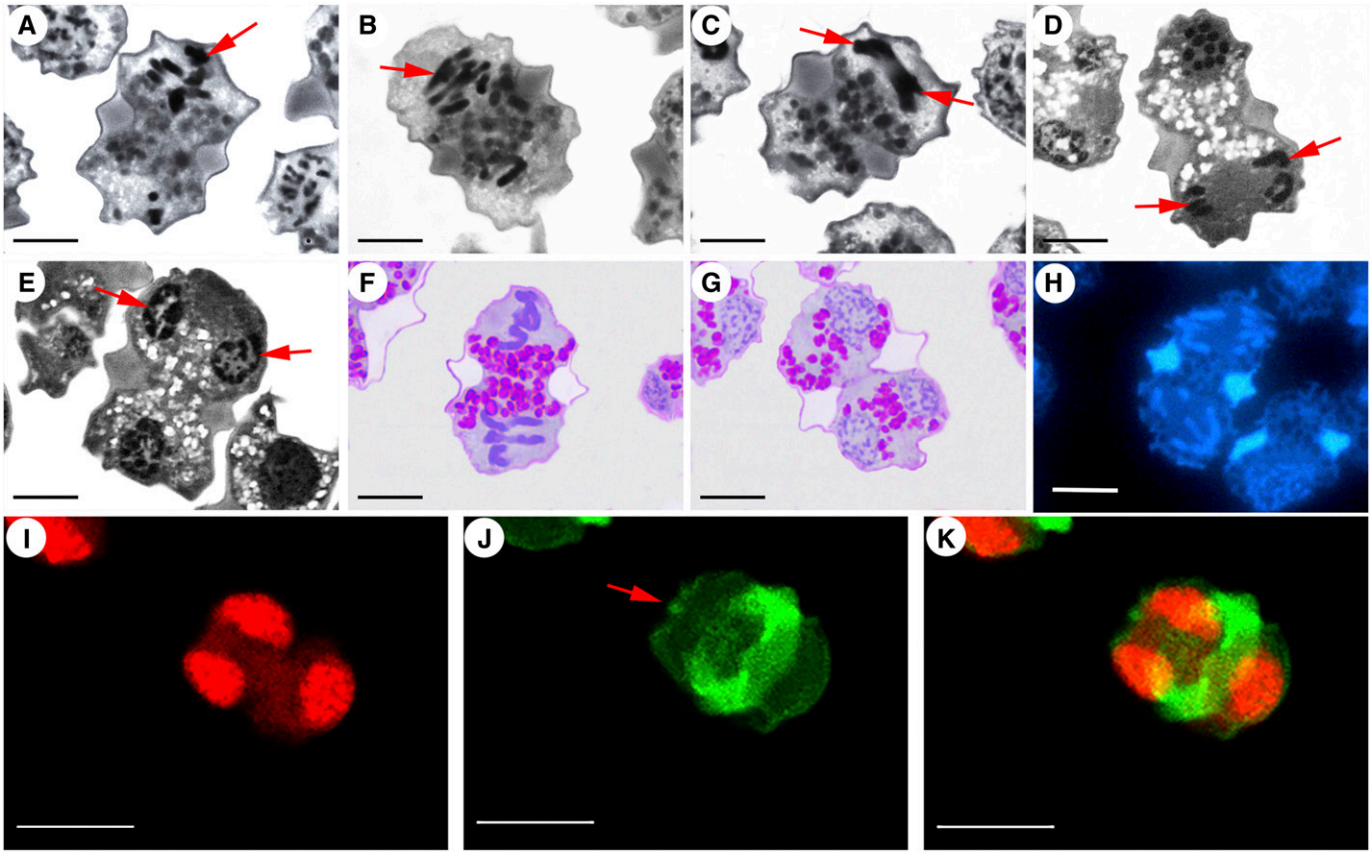

FIGURE 6 Microsporocytes at stages from metaphase II to telophase II. (A–E) Semithin sections stained with toluidine blue O. (A–C) Microsporocytes appeared to be at slightly different stages of anaphase II when chromosomes (arrows) were moving toward the opposite poles. (D, E) Telophase II, with chromosomes (arrows) at opposite poles in (D) and with newly formed nuclei in (E). (F, G) Semithin sections after PAS reaction and haematoxylin staining. (F) Plastids containing starch grains at the equatorial plane at metaphase II. (G) Plastids containing starch grains had migrated to the vicinities of the newly formed nuclei at telophase II. (H) Semithin section stained with DAPI and aniline blue showing the chromosomes at late anaphase II or early telophase II and the extent of callose deposition in the cell wall. (I–K) Images constructed by stacking the *z*-series of CLSM images, showing a three-dimensional view of the callose deposition. (I) Propidium iodide staining, showing nuclei at telophase II. (J) Aniline blue staining (false-colored to green), showing the callose deposition throughout the wall of the same cell in (I). (K) Merged image of (I) and (J). The pattern of callose deposition (e.g., the callose ring and the small area indicated by the arrow in (J)) at these stages remained the same as that at earlier stages (Fig. 4), except that the overall amount of callose in the wall seemed to have increased moderately. Scale bars: A–H = 10 μm, I–K = 20 μm.

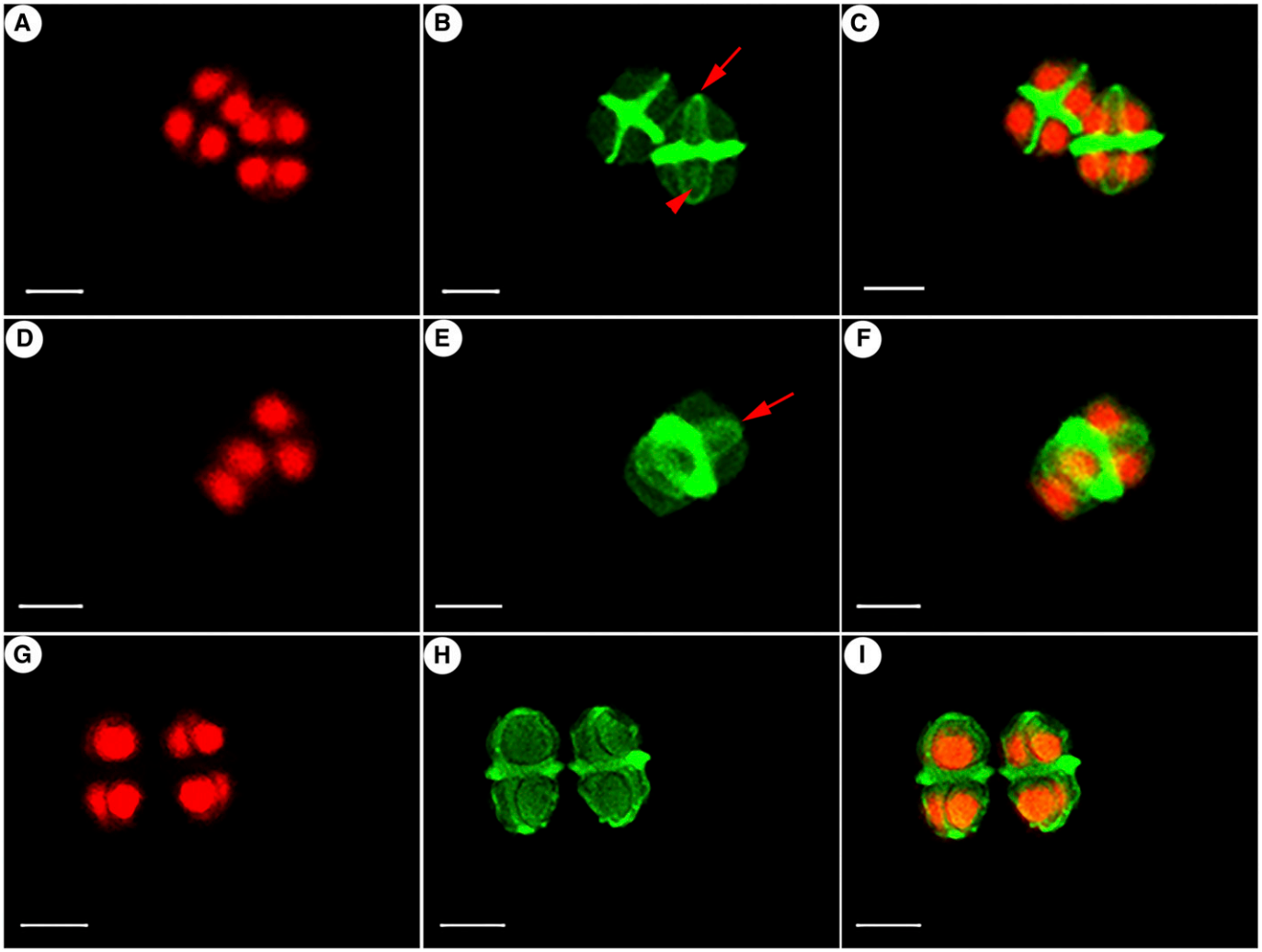

FIGURE 7 Completion of cytokinesis for tetrad formation. (A–F) Images constructed by stacking the *z*-series of CLSM images to show a three-dimensional view of callose deposition. As described earlier, the three images in each row are propidium iodide-stained, aniline blue-stained, and one merged from the preceding two images, respectively. (A–C) The second callose ring (arrow) was formed in a plane perpendicular to that of the first callose ring after telophase II. Some callose deposition was observed in the center of the plane that contained the second callose ring (arrowhead), indicating the initiation of a cell plate in the interior of the cytoplasm, which was going to join the second callose ring at the cell periphery. The first callose ring in the same microsporocyte had developed into a thick wall, and a nearby tetragonal tetrad had already formed with two walls in the planes in which the two callose rings used to reside. (D–F) A developing tetrad when both callose rings existed. (G–I) Two developing tetrads, showing that a solid callose wall had formed in the location specified by the first callose ring, and the cell plates had yet to make the connections with the second callose ring (note the gaps between the circular cell plates and the second callose ring). Scale bars = 20 μm.

similar to those as the major hallmarks of cytokinesis during *Arabidopsis* microsporogenesis were detected (Fig. 8). In particular, in addition to the wall stub, mini-phragmoplasts, wide tubules, wide tubular networks, and more continuous cell plates were found at the division planes in microsporocytes at slightly different stages (Fig. 8B–E). At maturity, the callose walls of a tetrad, except that from the first callose ring, were uniform in thickness (Figs. 8F, 9A–F). Starch grains were abundant around the nuclei in a newly formed

FIGURE 8 Transmission electron micrographs of developing and mature tetrads. (A) Tetrad showing the two callose rings without apparent cell plate formation. (B–E) Developing tetrads at slightly different stages. (B) Discontinuous, wide tubules aligned at a division plane. (C) Mini-phragmoplasts and wide tubular networks were at a division plane and near a callose ring. (D) Cell plate with a peripheral mini-phragmoplast was at a division plane. The cell plate consisted of regions that resembled the already formed callose wall in electron density. (E) A cell plate spanned the entire length of the division plane, and the callose ring seemed to be in a process of making a connection with the cell plate (rectangle). (F) Mature tetrad possessed continuous callose walls. C: callose ring; CP: cell plate; CW: cell wall; ER: endoplasmic reticulum; M: mitochondrion; MP: mini-phragmoplast; N: nucleus; SG: starch grain; V: vesicle; WT: wide tubule; WTN: wide tubular network.

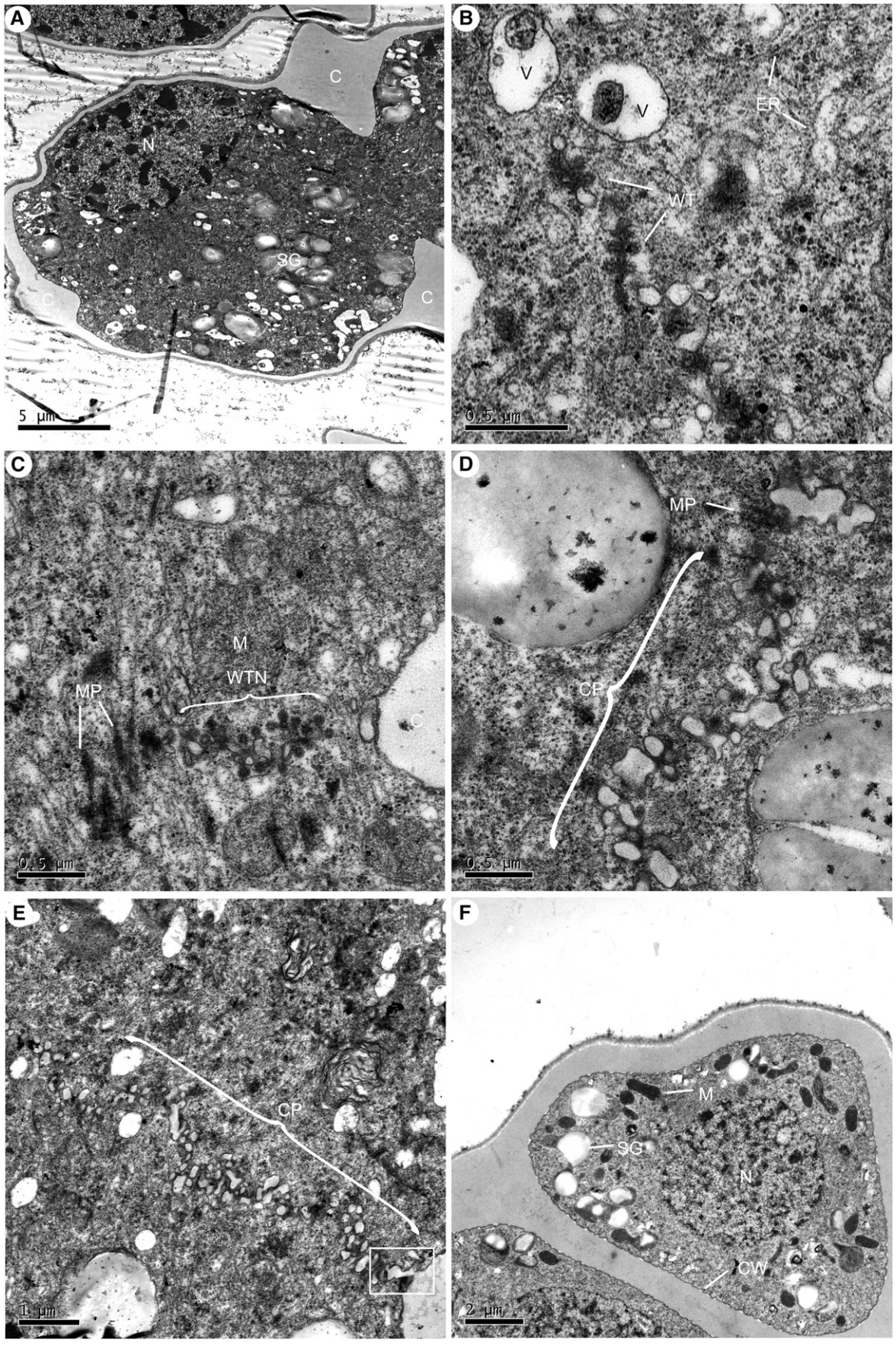

tetrad (Fig. 9D), but diminished in number later (Fig. 9E). The tetrad stage lasted for about 2 d. Shortly after the tetrad wall had broken down, free microspores had little callose in their walls (Fig. 9G–I).

DISCUSSION

***Cytokinesis in microsporogenesis in* M. communis**—An electron tomographic analysis by Otegui and Staehelin (2004) revealed the cellular structures apparently involved in building a complete cell plate during cytokinesis in microsporogenesis in *Arabidopsis thaliana*. These structures include mini-phragmoplasts, vesicles, wide tubules, wide tubular networks, and convoluted sheets with and without a cell wall stub. The wide tubules initially result from fusion of the vesicles, and the wide tubular networks result from connections of the wide tubules. At the cytokinetic site on the parent cell wall, the convoluted sheets without an apparent cell wall stub first appear, and later a cell wall stub appears with the convoluted sheets at its leading edges. In microsporogenesis in *M. communis*, however, two cell wall stubs or ACWIs in the form of callose rings occur after the two nuclear divisions, respectively, without the concurrent formation of mini-phragmoplasts, vesicles, wide tubules, or wide tubular networks (Fig. 10B). These observations indicate that cytokinesis in microsporogenesis in *M. communis* occurs in two steps, first at the cell periphery, and then, after a significant delay, in the cell interior. Even though intermediate cytokinetic structures in the cell interior were not examined in previous studies of several other

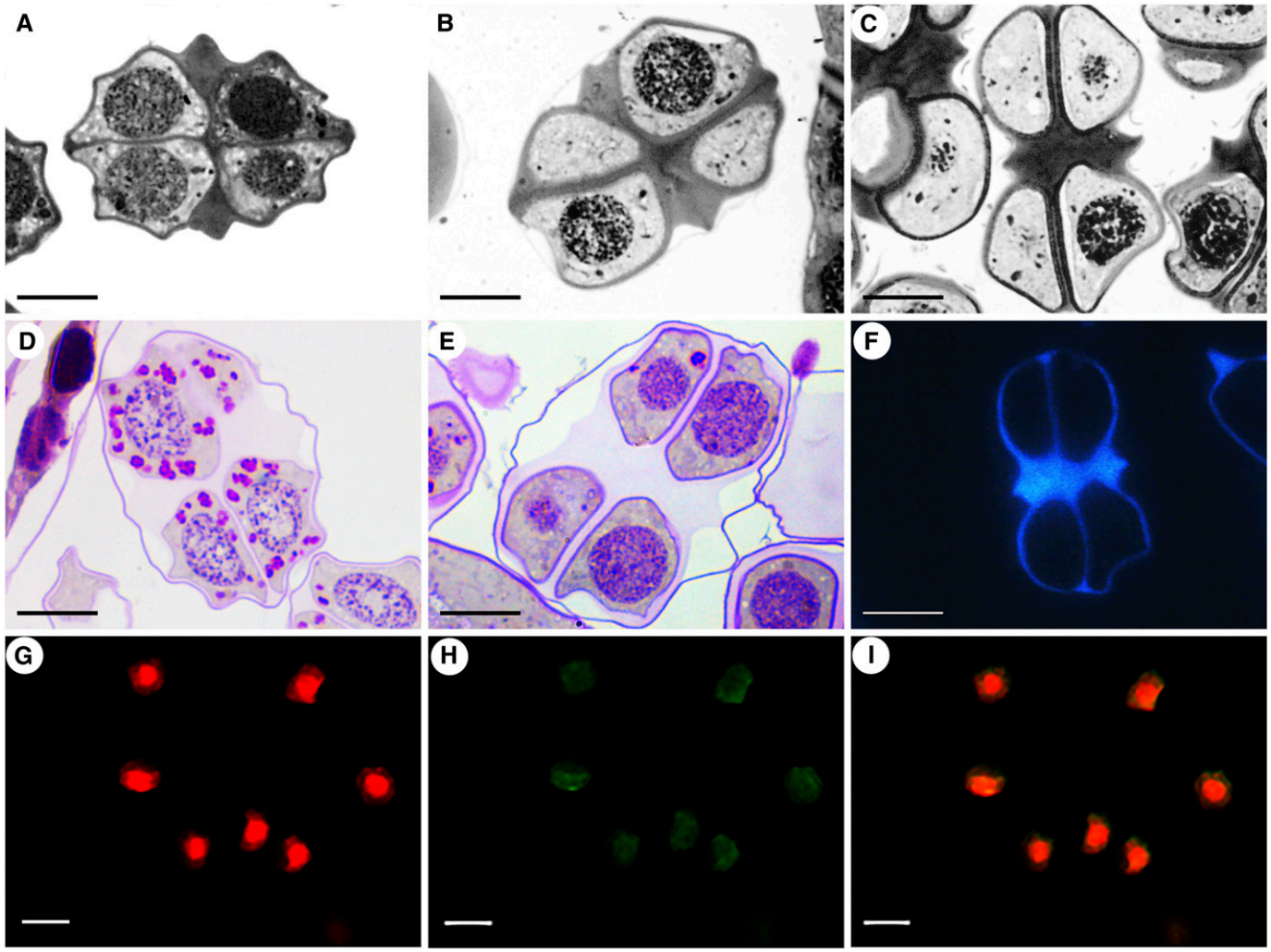

FIGURE 9 Thicknesses of callose walls of mature tetrads and free uninucleate microspores. (A–C) Semithin sections stained with toluidine blue O. (A–C) Tetrads with fully developed callose walls. Parts of the transverse wall formed from the first callose ring were much thicker than the rest of the transverse wall and the other cell walls of the same tetrad. (D, E) Semithin sections after PAS and haematoxylin staining. (D) Starch grains around the nuclei. (E) Starch grains largely absent, suggesting that (E) was at a later stage than (D). Tetrads in (D) and (E) also differed in their nuclear staining for haematoxylin. (F) Semithin section stained with DAPI and aniline blue, showing the different thicknesses of the callose walls of a tetrad (no nuclei were in section). (G–I) Images constructed by stacking the *z*-series of CLSM images, showing a three-dimensional view of the callose walls. As described earlier, the three images are propidium iodide-stained, aniline blue-stained, and one merged from the preceding two images, respectively. These uninucleate microspores had been released from the callose walls of the tetrads, and each appeared to have a thin callose wall. Scale bars: A–F = 10 µm, G–I = 20 µm.

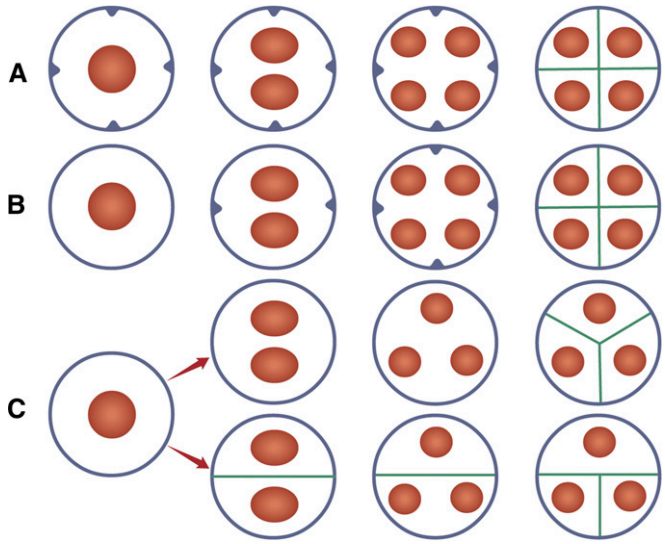

FIGURE 10 Schematic representation of cytokinesis in major land plants. (A) Bryophytes and at least some ferns with simultaneous formation of advance cell wall ingrowths (ACWIs). (B) Cycads and *Magnolia* with sequential formation of ACWIs. (C) Noncycad gymnosperms and non-*Magnolia* angiosperms without ACWIs, showing both simultaneous cytokinesis (upper arrow) and successive cytokinesis (lower arrow). Not all possible tetrad forms are shown. Blue: parental cell walls with or without ACWIs; brown: nuclei; and green: newly formed cell walls.

cycad species, a localized cell-wall-thickening region corresponding to the callose ring and a future cytokinetic site was observed during the period between the first and second nuclear divisions (Singh, 1978; Audran, 1981; Zhang et al., 2012). ACWIs at a future cytokinetic site in microsporogenesis are thus likely a general phenomenon in cycads. It is noted here that microsporogenic cytokinesis in cycads has been described as either simultaneous (Singh, 1978; Audran, 1981; Zhang et al., 2012), successive (Baird, 1939; De Silva and Tambiah, 1952; Rao, 1961; Wu et al., 1995), or mixed (Ouyang et al., 2004) based on limited light microscopy studies. Based on this study and reevaluation of the literature, we argue that the cytokinesis type in microsporogenesis in cycads is most closely related to the intermediate type as exemplified by *Magnolia*.

***Comparison of cytokinesis in sporogenesis in major groups of land plants*—**Cytokinesis in sporogenesis in bryophytes and a fern species also occurs with cell wall stub (protrusion) formation in advance of the centrifugal phragmoplast-based cell plate formation (Sheffield et al., 1983; Brown and Lemmon, 2013). In contrast to cycads, two rings of callose wall protrusions form even before the first nuclear division in these plants, and they specify the locations where the parental cell wall will join with the cell plates after the second nuclear division (Fig. 10A, B). On the other hand, ACWIs at future cytokinetic sites have not been observed in gymnosperms other than cycads and angiosperms other than *Magnolia*. In the majority of seed plants, wall stub formation is closely coupled with cell plate formation in both simultaneous cytokinesis and successive cytokinesis (Fig. 10C). As a comparison, in *Ginkgo biloba*, cytokinesis in microsporogenesis appears to be simultaneous without ACWIs (Brown and Lemmon, 2005; Lu et al., 2011). ACWIs are likely to occur widely in nonseed land plants (Sheffield et al., 1983; Brown and Lemmon, 2013) but they are limited to only a few ancient lineages of seed plants. Interestingly, callose-based cell wall ingrowths independent of a phragmoplast and preceding phragmoplast-dependent cell plate formation were also observed in the initial phase of cellularization of wheat endosperm and were recognized as a process similar to the cleavage process of lower plant cells (Morrison and O'Brien, 1976). These observations suggest that ACWIs may be an ancient feature of microsporogenesis in seed plants, coupled with the ancestral feature of simultaneous cytokinesis as proposed by Nadot et al. (2008). If so, an evolutionary trend in microsporogenic cytokinesis seems to be the increasing coordination between the cell wall ingrowths at the cell periphery and cell plate formation in the cell interior. How this coordination is accomplished at the molecular level is an important question in the regulation of cytokinesis in plants. Cycads, in comparison with other seed plants, provide a special system for addressing this question since the two processes are temporally uncoupled during cytokinesis in microsporogenesis.

There is a vast amount of literature on microsporogenesis in diverse species, but ACWIs have not been the focus of previous investigations. Moreover, the absence of ACWIs in some previous studies may be inconclusive due to the lack of the appropriate meiotic stages. To assess how widely ACWIs occur in meiosis in plants, sufficient meiotic stages should be investigated in diverse plant species whose microsporogenesis or sporogenesis either has not been investigated or requires further examination.

***Spatial and temporal control of the callose deposition*—**Callose deposition is a common event during meiosis in plants (Singh, 1978; Johri, 1984; Bhatia and Malik, 1996; Lü et al., 2003; Lu et al., 2011; Zhang et al., 2012). In *M. communis*, two callose rings form at the sites where future cell plates will join the parental cell wall in advance of the mini-phragmoplast-based process of cell plate formation in the interior of the cell. There is only a slight accumulation of callose in other parts of the wall beyond the callose rings. Only at the tetrad stage is the callose wall thickened throughout the cell surface (e.g., Fig. 8F compared with Fig. 8A). How callose deposition is temporally and spatially controlled is a curious case in cellular regulation. Actin filaments and microtubules have been shown to control, respectively, the transport and positioning of callose synthase in tobacco pollen tubes (Cai et al., 2011). A similar mechanism may spatially control callose deposition during microsporogenesis of *M. communis* even though currently there is no experimental evidence supporting this idea.

ACKNOWLEDGEMENTS

The authors thank Professor Letian Chen at South China Agricultural University for help with the CLSM work and Xuan Lun and Chuanhe Liu at South China Agricultural University for technical assistance with the transmission electron microscopy work. This work was supported by a grant (No. 31200147) from the Natural Science Foundation of China and a grant (SSTLAB-2014-01) from the Public Subject Foundation from Shenzhen Key Laboratory of Southern Subtropical Plant Diversity, Fairylake Botanical Garden, Chinese Academy of Sciences.

LITERATURE CITED

Anderson, E. D., and J. N. Owens. 2000. Microsporogenesis, pollination, pollen germination and male gametophyte development in *Taxus brevifolia*. *Annals of Botany* 86: 1033–1042.

Audran, J. C. 1981. Pollen and tapetum development in *Ceratozamia mexicana* (cycadaceae): Sporal origin of the exinic sporopollenin in cycads. *Review of Palaeobotany and Palynology* 33: 315–346.

Baird, A. M. 1939. A contribution to the life history of *Macrozamia riedlei*. *Journal of the Royal Society of Western Australia* 25: 153–175.

Balasubramanian, M. K., E. Bi, and M. Glotzer. 2004. Comparative analysis of cytokinesis in budding yeast, fission yeast and animal cells. *Current Biology* 14: R806–R818.

Bhatia, D. S., and C. P. Malik. 1996. Significance of callose in reproduction of higher plants with special reference to male gametophyte. *In* C. P. Malik [ed.], Pollen–spore research emerging strategies. Advances in pollen–spore research, vol. 21, 221–240. Today and Tomorrow's Printers and Publishers, New Delhi, India.

Bowe, L. M., G. Coat, and C. W. dePamphilis. 2000. Phylogeny of seed plants based on all three genomic compartments, extant gymnosperms are monophyletic and Gnetales' closest relatives are conifers. *Proceedings of the National Academy of Sciences, USA* 97: 4092–4097.

Brenner, E. D., D. W. Stevenson, and R. W. Twigg. 2003. Cycads: Evolutionary innovations and the role of plant-derived neurotoxins. *Trends in Plant Science* 8: 446–452.

Brown, R. C., and B. E. Lemmon. 1992. Control of division plane in normal and griseofulvin-treated microsporocytes of *Magnolia*. *Journal of Cell Science* 103: 1031–1038.

Brown, R. C., and B. E. Lemmon. 2001. The cytoskeleton and spatial control of cytokinesis in the plant life cycle. *Protoplasma* 215: 35–49.

Brown, R. C., and B. E. Lemmon. 2005. γ-Tubulin and microtubule organization during microsporogenesis in *Ginkgo biloba*. *Journal of Plant Research* 118: 121–128.

Brown, R. C., and B. E. Lemmon. 2013. Sporogenesis in bryophytes: Patterns and diversity in meiosis. *Botanical Review* 79: 178–280.

Cai, G., C. Faleri, C. Del Casino, A. M. C. Emons, and M. Cresti. 2011. Distribution of callose synthase, cellulose synthase, and sucrose synthase in tobacco pollen tube is controlled in dissimilar ways by actin filaments and microtubules. *Plant Physiology* 155: 1169–1190.

Chaw, S. M., C. L. Parkinson, Y. Cheng, T. M. Vincent, and J. D. Palmer. 2000. Seed plant phylogeny inferred from all three plant genomes: Monophyly of extant gymnosperms and origin of Gnetales from conifers. *Proceedings of the National Academy of Sciences, USA* 97: 4086–4091.

De Silva, B. L. T., and M. S. Tambiah. 1952. A contribution to the life history of *Cycas rumphii* Miq. *Ceylon Journal of Science* 12A: 1–22.

Farr, C. H. 1918. Cell division by furrowing in *Magnolia*. *American Journal of Botany* 5: 379–395.

Field, C., R. Li, and K. Oegema. 1999. Cytokinesis in eukaryotes: A mechanistic comparison. *Current Opinion in Cell Biology* 11: 68–80.

Furness, C. A., P. J. Rudall, and F. B. Sampson. 2002. Evolution of microsporogenesis in angiosperms. *International Journal of Plant Sciences* 163: 235–260.

Glotzer, M. 1997. The mechanism and control of cytokinesis. *Current Opinion in Cell Biology* 9: 815–823.

Gunning, B. E. S. 1982. The cytokinetic apparatus: Its development and spatial regulation. *In* C. W. Lloyd [ed.], The cytoskeleton in plant growth and development, 229–292. Academic Press, New York, New York, USA.

Johri, B. M. 1984. Embryology of angiosperms. Springer-Verlag, Berlin, Germany.

Jürgens, G. 2005. Cytokinesis in higher plants. *Annual Review of Plant Biology* 56: 281–299.

Lü, S., Y. Li, Z. Chen, and J. Lin. 2003. Pollen development in *Picea asperata* Mast. *Flora* 198: 112–117.

Lu, Y., L. Wang, D. Wang, Y. Wang, M. Zhang, B. Jin, and P. Chen. 2011. Male cone morphogenesis, pollen development and pollen dispersal mechanism in *Ginkgo biloba* L. *Canadian Journal of Plant Science* 91: 971–981.

Maheshwari, P. 1935. Contributions to the morphology of *Ephedra foliata*, Boiss. I: The development of the male and female gametophytes. *Proceedings of the Indian Academy of Sciences, B* 1: 586–606.

Mineyuki, Y. 1999. The preprophase band of microtubules: Its function as a cytokinetic apparatus in higher plants. *International Review of Cytology* 187: 1–49.

Moitra, A., and S. P. Bhatnagar. 1982. Ultrastructure, cytochemical, and histochemical studies on pollen and male gamete development in gymnosperms. *Gamete Research* 5: 71–112.

Morrison, I. N., and T. P. O'brien. 1976. Cytokinesis in the developing wheat grain; division with and without a phragmoplast. *Planta* 130: 57–67.

Nadot, S., C. A. Furness, J. Sannier, L. Penet, S. Triki-Teutroy, B. Albert, and A. Ressayre. 2008. Phylogenetic comparative analysis of microsporogenesis in angiosperms with a focus on monocots. *American Journal of Botany* 95: 1426–1436.

Otegui, M. S., and L. A. Staehelin. 2004. Electron tomographic analysis of postmeiotic cytokinesis during pollen development in *Arabidopsis thaliana*. *Planta* 218: 501–515.

Ouyang, H., Y. Li, S. Zhang, N. Li, and H. Wu. 2004. Microsporogenesis of *Cycas elongata* and its systematic implication. *Acta Phytotaxonomica Sinica* 42: 500–512.

Pickett-Heaps, J. D., B. E. Gunning, R. C. Brown, B. E. Lemmon, and A. L. Cleary. 1999. The cytoplast concept in dividing plant cells: Cytoplasmic domains and the evolution of spatially organized cell division. *American Journal of Botany* 86: 153–172.

Rao, L. N. 1961. Life history of *Cycas circinalis* L. (part I). Microsporogenesis, male and female gametophytes and spermatogenesis. *Journal of the Indian Botanical Society* 40: 601–619.

Sampson, F. B. 1969a. Cytokinesis in pollen mother cells of angiosperms, with emphasis on *Laurelia novae-zelandiae* (Monimiaceae). *Cytologia* 34: 627–634.

Sampson, F. B. 1969b. Studies on the Monimiaceae. III. Gametophyte development of *Laurelia novae-zelandiae* A. Cunn. (subfamily Atherospermoideae). *Australian Journal of Botany* 17: 425–439.

Sauquet, H., J. A. Doyle, T. Scharaschkin, T. Borsch, K. W. Hilu, L. W. Chatrou, and A. Le Thomas. 2003. Phylogenetic analysis of Magnoliales and Myristicaceae based on multiple data sets: Implications for character evolution. *Botanical Journal of the Linnean Society* 142: 125–186.

Sheffield, E., S. Laird, and P. R. Bell. 1983. Ultrastructural aspects of sporogenesis in the apogamous fern *Dryopteris borreri*. *Journal of Cell Science* 63: 125–134.

Singh, H. 1978. Embryology of gymnosperms. Gebrüder Borntraeger, Berlin, Germany.

Wang, Y., and M. Yang. 2006. The ARABIDOPSIS SKP1-LIKE1 (ASK1) protein acts predominately from leptotene to pachytene and represses homologous recombination in male meiosis. *Planta* 223: 613–617.

Wang, Y., and M. Yang. 2014. Loss-of-function mutants and overexpression lines of the Arabidopsis cyclin *CYCA1; 2/Tardy Asynchronous Meiosis* exhibit different defects in prophase-I meiocytes but produce the same meiotic products. *PLoS ONE* 9: e113348.

Worrall, D., D. L. Hird, R. Hodge, W. Paul, J. Draper, and R. Scott. 1992. Premature dissolution of the microsporocyte callose wall causes male sterility in transgenic tobacco. *Plant Cell* 4: 759–771.

Wu, X., P. Li, and C. Li. 1995. Investigation on the reproductive biology of *Cycas panzhihuaensi*—Microsporogenesis and development of pollen grain. *Journal of Sichuan University* 32: 69–76 (Natural Science Edition).

Zhang, H., H. Ouyang, J. Du, S. Zhang, Y. Li, and H. Wu. 2012. Microsporogenesis of *Cycas* and its systematic implications. *Journal of Systematics and Evolution* 50: 125–134.

Zhang, S., W. Yang, Y. Qi, M. Li, J. Wang, X. Sun, X. Wang, and L. Qi. 2008. Development of male gametophyte of *Larix leptolepis* Gord. with emphasis on diffuse stage of meiosis. *Plant Cell Reports* 27: 1687–1696.